Electronic Supplementary Material (ESI) for Journal of Materials Chemistry A.
This journal is © The Royal Society of Chemistry 2020

Supplementary Information

Highly selective aerobic oxidation of methane to methanol over gold decorated zinc oxide via photocatalysis

Wencai Zhou,[a] Xueying Qiu,[a] Yuheng Jiang,[a] Yingying Fan,[*ab] Shilei Wei,[b] Dongxue Han,[*b] Li Niu,[b] Zhiyong Tang[a]

[*]Corresponding author. Email: dxhan@gzhu.edu.cn; ccyyfan@gzhu.edu.cn

[a]Chinese Academy of Sciences (CAS) Key Laboratory of Nanosystem and Hierarchy Fabrication, CAS Center for Excellence in Nanoscience, National Center for Nanoscience and Technology, Beijing 100190, China.

[b]Center for Advanced Analytical Science, School of Chemistry and Chemical Engineering c/o School of Civil Engineering, Guangzhou University, Guangzhou 510006, P. R. China.

Sample ID:	1							a
Replicates								
Replicate	1							
IS	Analyte	Mass	Meas. Intensity	Net Intensity	Concentration	Sample Unit		
	Au	197	1595.4	1289.641	0.1	ug/L		
Replicate	2							
IS	Analyte	Mass	Meas. Intensity	Net Intensity	Concentration	Sample Unit		
	Au	197	1650.1	1344.314	0.11	ug/L		
Replicate	3							
IS	Analyte	Mass	Meas. Intensity	Net Intensity	Concentration	Sample Unit		
	Au	197	1676.1	1370.317	0.11	ug/L		
Summary								
IS	Analyte	Mass	Meas. Intens. Mean	Net Intens. Mean	Conc. Mean	Conc. SD	Conc. RSD	Report Unit
	Au	197	1640.5	1334.8	0.11	0.003	3.09	ug/L

1.30 mg $Au_{0.08}$/ZnO

Quantitative Analysis - Comprehensive Report								
Sample ID:	2							b
Replicates								
Replicate	1							
IS	Analyte	Mass	Meas. Intensity	Net Intensity	Concentration	Sample Unit		
	Au	197	3558.4	3252.662	0.26	ug/L		
Replicate	2							
IS	Analyte	Mass	Meas. Intensity	Net Intensity	Concentration	Sample Unit		
	Au	197	3260.4	2954.591	0.23	ug/L		
Replicate	3							
IS	Analyte	Mass	Meas. Intensity	Net Intensity	Concentration	Sample Unit		
	Au	197	3321.7	3015.938	0.24	ug/L		
Summary								
IS	Analyte	Mass	Meas. Intens. Mean	Net Intens. Mean	Conc. Mean	Conc. SD	Conc. RSD	Report Unit
	Au	197	3380.2	3074.4	0.24	0.012	5.12	ug/L

1.60 mg $Au_{0.15}$/ZnO

Quantitative Analysis - Comprehensive Report								
Sample ID:	3							c
Replicates								
Replicate	1							
IS	Analyte	Mass	Meas. Intensity	Net Intensity	Concentration	Sample Unit		
	Au	197	15254.8	14949.026	1.18	ug/L		
Replicate	2							
IS	Analyte	Mass	Meas. Intensity	Net Intensity	Concentration	Sample Unit		
	Au	197	15432.3	15126.55	1.19	ug/L		
Replicate	3							
IS	Analyte	Mass	Meas. Intensity	Net Intensity	Concentration	Sample Unit		
	Au	197	15252.1	14946.357	1.18	ug/L		
Summary								
IS	Analyte	Mass	Meas. Intens. Mean	Net Intens. Mean	Conc. Mean	Conc. SD	Conc. RSD	Report Unit
	Au	197	15313.1	15007.3	1.18	0.008	0.69	ug/L

3.88 mg $Au_{0.30}$/ZnO

Sample ID:	4							d
Replicates								
Replicate	1							
IS	Analyte	Mass	Meas. Intensity	Net Intensity	Concentration	Sample Unit		
	Au	197	14757.6	14451.838	1.14	ug/L		
Replicate	2							
IS	Analyte	Mass	Meas. Intensity	Net Intensity	Concentration	Sample Unit		
	Au	197	14444.6	14138.851	1.11	ug/L		
Replicate	3							
IS	Analyte	Mass	Meas. Intensity	Net Intensity	Concentration	Sample Unit		
	Au	197	14329.2	14023.402	1.1	ug/L		
Summary								
IS	Analyte	Mass	Meas. Intens. Mean	Net Intens. Mean	Conc. Mean	Conc. SD	Conc. RSD	Report Unit
	Au	197	14510.5	14204.7	1.12	0.017	1.56	ug/L

1.56 mg $Au_{0.75}$/ZnO

Sample ID:	5							e
Replicates								
Replicate	1							
IS	Analyte	Mass	Meas. Intensity	Net Intensity	Concentration	Sample Unit		
	Au	197	44631.6	44325.83	3.49	ug/L		
Replicate	2							
IS	Analyte	Mass	Meas. Intensity	Net Intensity	Concentration	Sample Unit		
	Au	197	44079.2	43773.452	3.45	ug/L		
Replicate	3							
IS	Analyte	Mass	Meas. Intensity	Net Intensity	Concentration	Sample Unit		
	Au	197	44095.3	43789.501	3.45	ug/L		
Summary								
IS	Analyte	Mass	Meas. Intens. Mean	Net Intens. Mean	Conc. Mean	Conc. SD	Conc. RSD	Report Unit
	Au	197	44268.7	43962.9	3.46	0.025	0.72	ug/L

2.24 mg $Au_{1.57}$/ZnO

Sample ID:	Au1.79							f
Replicates								
Replicate	1							
IS	Analyte	Mass	Meas. Intensity	Net Intensity	Concentration	Sample Unit		
	Au	197	79790.2	79484.425	6.26	ug/L		
Replicate	2							
IS	Analyte	Mass	Meas. Intensity	Net Intensity	Concentration	Sample Unit		
	Au	197	81566.2	81260.413	6.4	ug/L		
Replicate	3							
IS	Analyte	Mass	Meas. Intensity	Net Intensity	Concentration	Sample Unit		
	Au	197	80830.7	80524.917	6.34	ug/L		
Summary								
IS	Analyte	Mass	Meas. Intens. Mean	Net Intens. Mean	Conc. Mean	Conc. SD	Conc. RSD	Report Unit
	Au	197	80729	80423.3	6.33	0.07	1.11	ug/L

3.59 mg $Au_{1.79}$/ZnO

Fig. S1 ICP-OES results of the samples. (a) 1.30 mg of $Au_{0.08}$/ZnO, (b) 1.60 mg of $Au_{0.15}$/ZnO, (c) 3.88 mg of $Au_{0.3}$/ZnO, (d) 1.56 mg of $Au_{0.75}$/ZnO, (e) 2.24 mg of $Au_{1.57}$/ZnO and (f) 3.59 mg of $Au_{1.79}$/ZnO were dissolved in the mixed acid solutions for the concentration tests of Au species.

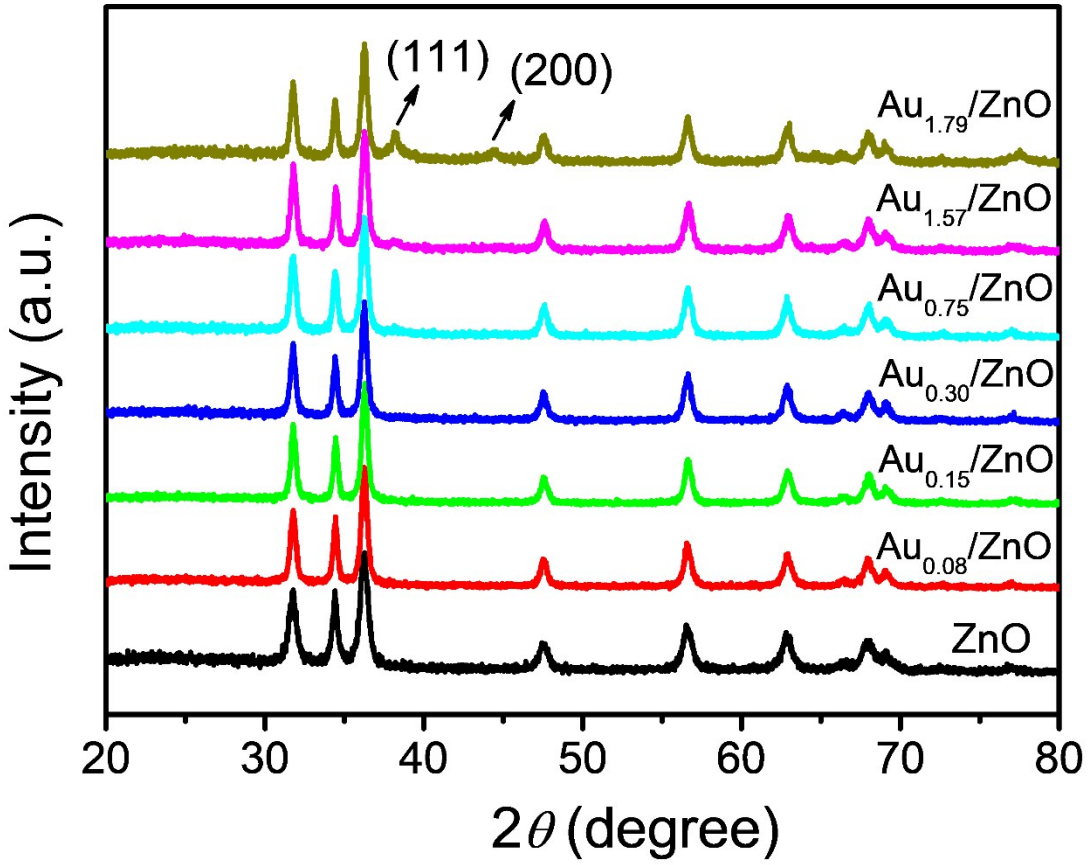

Fig. S2 XRD patterns of Au_x/ZnO (x = 0, 0.08, 0.15, 0.30, 0.75, 1.57 and 1.79).

To investigate the influences for crystal types by Au loading amounts, XRD patterns of Au_x/ZnO (x = 0, 0.08, 0.15, 0.30, 0.75, 1.57 and 1.79) are tested as shown in Fig.S2. However, in the cases of Au_x/ZnO (x = 0.08, 0.15, 0.30, 0.75 and 1.57), merely ZnO crystal peaks with no observation of Au are detected, which may be attributed to the trace loading amounts of Au. Until enhancing the Au loading amount to 1.79 %, obvious XRD peaks on Au (111) and Au (200) emerge as convincing proofs for Au deposition. Meanwhile, ZnO also remains the intact crystal structure in the sample of $Au_{1.79}$/ZnO.

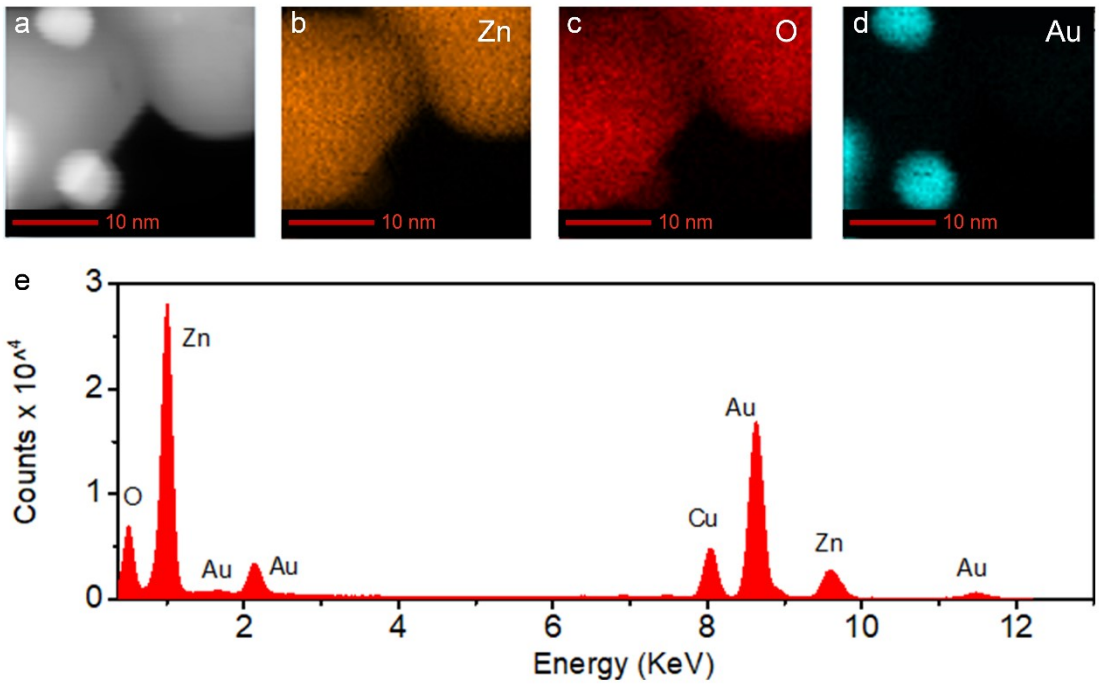

Fig. S3 (a) HAADF-STEM image and (b-d) corresponding element mapping of (b) Zn, (c) O and (d) Au over $Au_{0.75}$/ZnO. (e) EDX spectroscopy of $Au_{0.75}$/ZnO.

The successful synthesis of $Au_{0.75}$/ZnO can also been verified by the elements distributions of Zn (Fig. S3b), O (Fig. S3c) and Au (Fig. S3d) from the element mapping by high-angle annular dark field scanning transmission electron microscope (HAADF-STEM, Fig. S3a) and energy dispersive X-ray (EDX) spectroscopy (Fig. S3e).

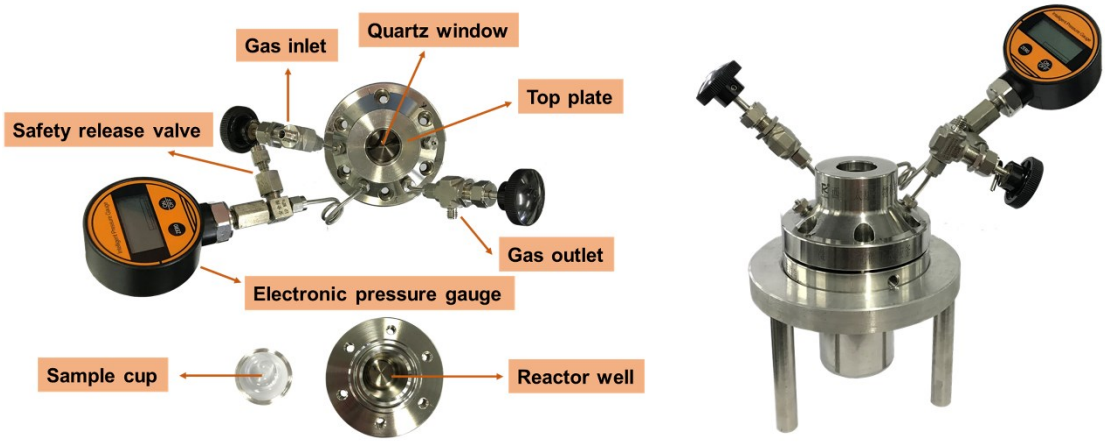

Fig. S4 Detailed configurations of high-pressure photocatalytic reactor for photocatalytic CH_4 oxidation.

The standard stainless-steel pressure vessel is assembled by a sample inner cup within a reactor well possessing 50 mL volume for reactant loading. A quartz window configurated is deposited in top plate to transit the external light source. Gas inlet and gas outlet are for reaction gas loading and unloading. Safety release valve is for security assurance. Electronic pressure gauge is for gas-pressure display.

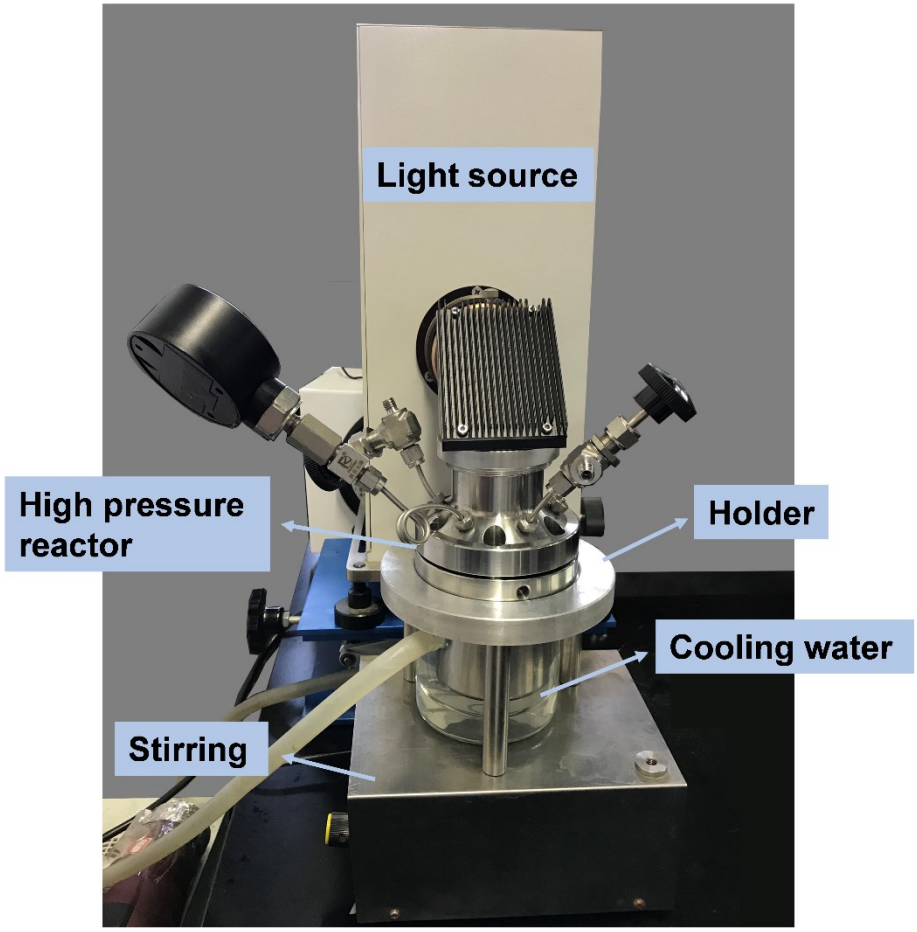

Fig. S5 Detailed illustration of the photocatalytic CH_4 oxidation reaction setup.

The photocatalytic CH_4 oxidation reaction setup contains light source, high pressure reactor, reactor holder, cooling water circulation and stirring apparatus.

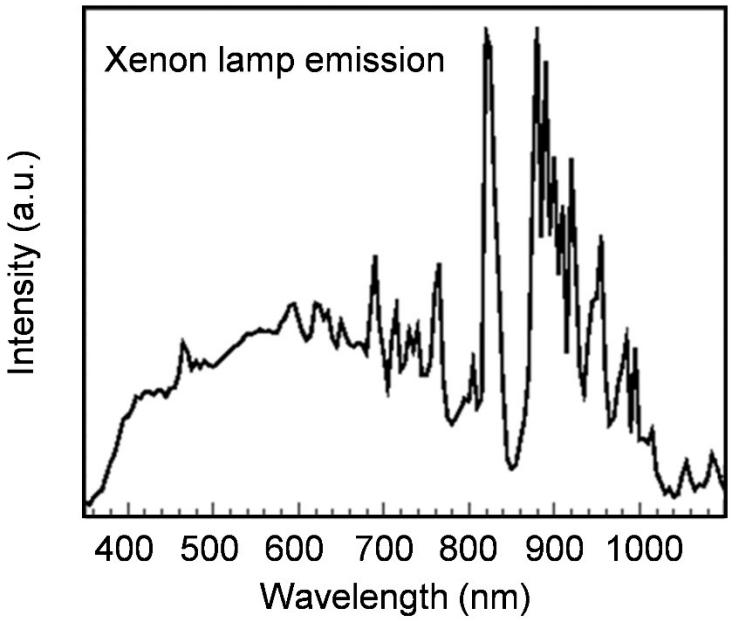

Fig. S6 Full light spectrum emission of Xenon lamp.

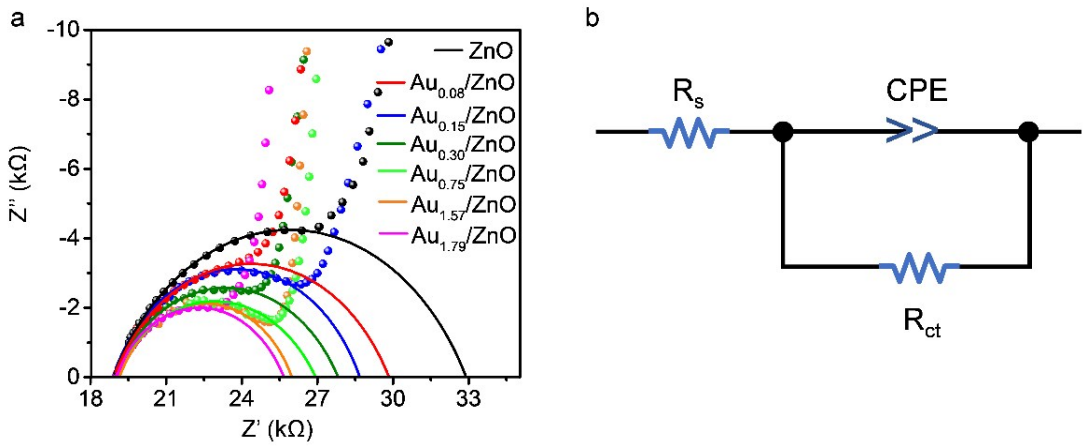

Fig. S7 (a) EIS plots of Au_x/ZnO (x= 0, 0.08, 0.15, 0.30, 0.75, 1.57 and 1.79) measured at 10 mV (vs. Ag/AgCl) in 1 M Na_2SO_4 solution under dark conditions. The semicircles of Nyquist plots have been fitted to demonstrate the accurate R_{ct} values with (b) corresponding equivalent circuit diagram. R_s, CPE and R_{ct} represent solution resistance, constant phase angle element and faraday impedance, respectively.

Electrochemical impedance spectroscopy (EIS) measurements were conducted in 1 M $NaSO_4$ solution by a CHI 760E electrochemical workstation as shown in Fig. S7. In order to accurately calculate the faraday impedance (R_{ct}), the semicircles of Nyquist plots have been fitted using the ZView software (Fig. S7a) with corresponding equivalent circuit diagram (Fig. S7b) sketched. As shown in Fig. S7a, along with the increasing amount of Au, the arc radius of Au_x/ZnO (x= 0, 0.08, 0.15, 0.30, 0.75, 1.57 and 1.79 wt%) decreases continuously, indicating the enhanced conductivity. Besides, through the equivalent circuit simulations, the R_{ct} values of ZnO, $Au_{0.08}$/ZnO, $Au_{0.15}$/ZnO, $Au_{0.30}$/ZnO, $Au_{0.75}$/ZnO, $Au_{1.57}$/ZnO and $Au_{1.79}$/ZnO are demonstrated to be 14.0, 10.9, 9.8, 8.9, 8.0, 7.2 and 7.0 kΩ, respectively. Compared to pristine ZnO, the smaller R_{ct} value of Au loaded ZnO represents the faster electronic transmission characteristic, which is benefit for the separation of photo-generated carriers.

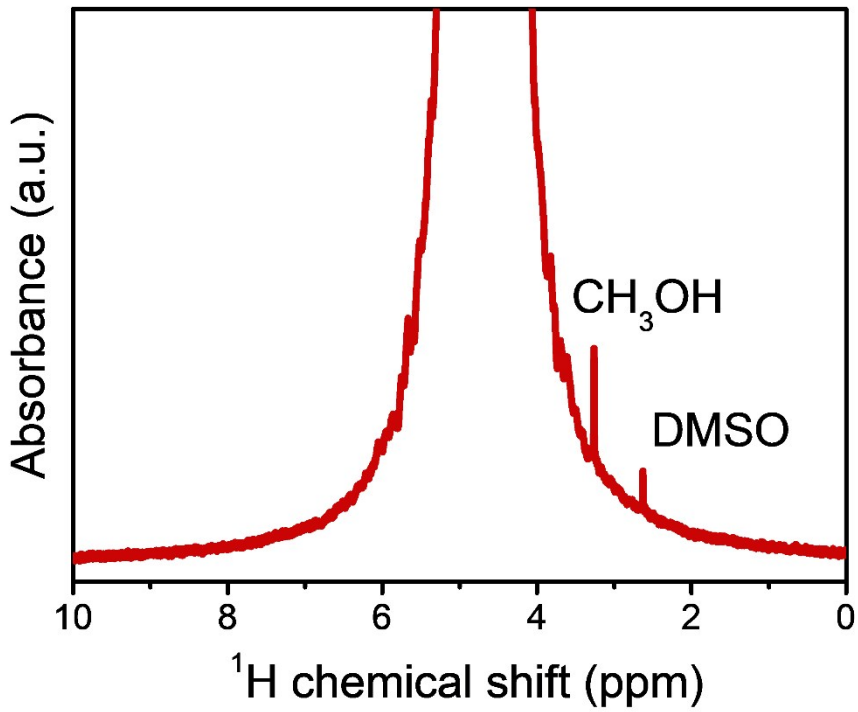

Fig. S8 ^{1}H NMR of CH_4 oxidation product over $Au_{0.75}/ZnO$. DMSO was added as internal standard in NMR test. ^{1}H NMR peak of CH_3OH is 3.28 ppm.

Only CH_3OH as product has been observed in photocatalytic CH_4 oxidation of $Au_{0.75}/ZnO$ from ^{1}H NMR spectrum. The chemical shift at 3.28 ppm is ^{1}H NMR characteristic peak of CH_3OH, no CH_3OOH peak (3.78 ppm) is observed.

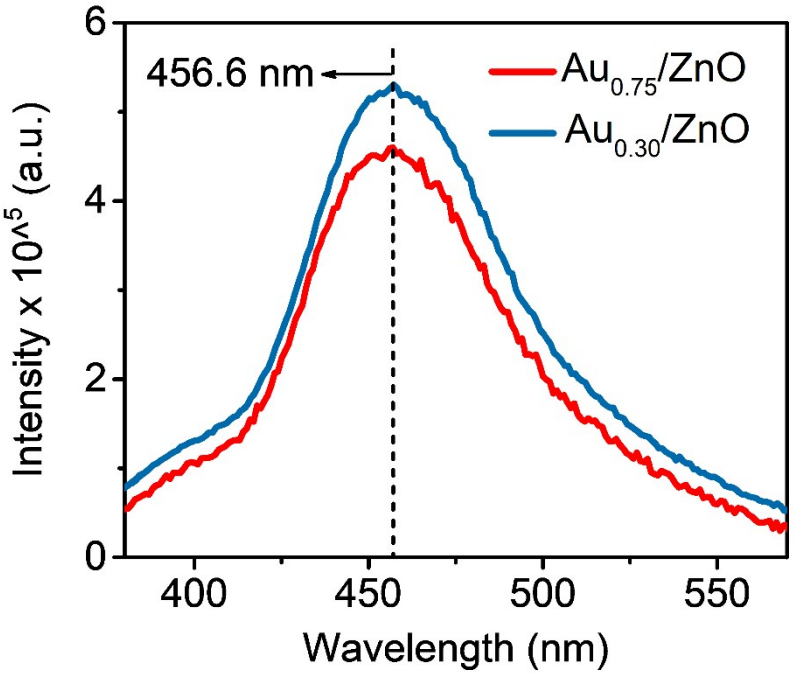

Fig. S9 Fluorescence spectra of 1 mM coumarin solution over $Au_{0.75}$/ZnO and $Au_{0.30}$/ZnO with the incorporation of 5 bar O_2. The fluorescence peaks are located at 456.6 nm under 332 nm excitation.

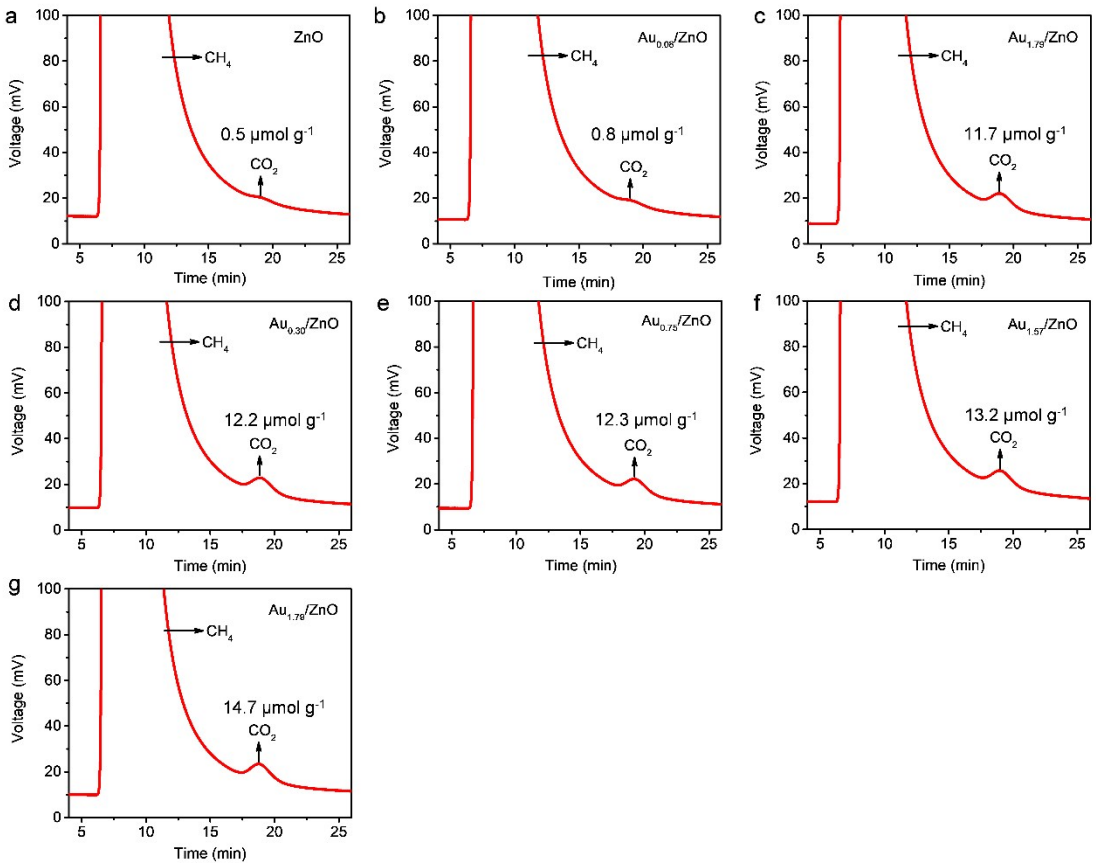

Fig. S10 GC spectra of CO_2 produced over (a) ZnO, (b) $Au_{0.08}$/ZnO, (c) $Au_{0.15}$/ZnO, (d) $Au_{0.30}$/ZnO, (e) $Au_{0.75}$/ZnO, (f) $Au_{1.57}$/ZnO and (g) $Au_{1.79}$/ZnO in photocatalytic CH_4 conversion.

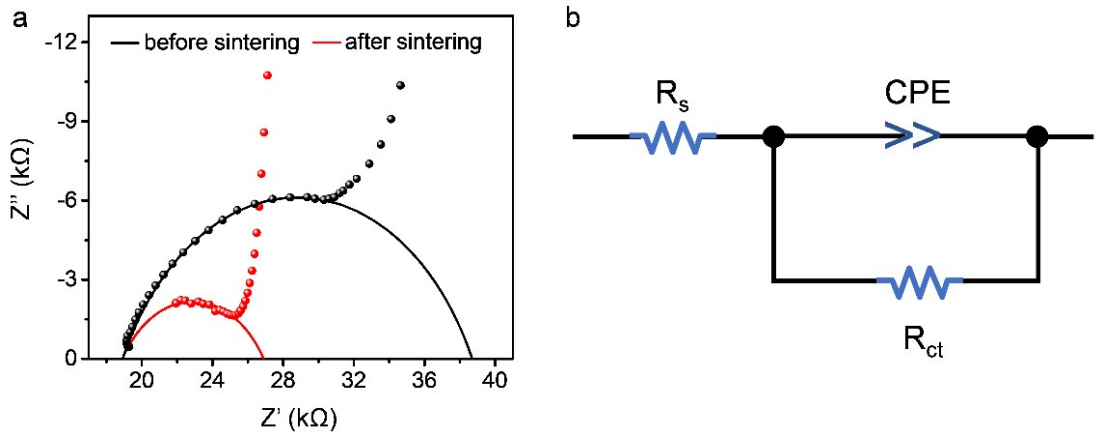

Fig. S11 (a) EIS plots of $Au_{0.75}$/ZnO before and after 500 °C calcination, which have been measured at 10 mV (vs. Ag/AgCl) in 1 M Na_2SO_4 solution under dark conditions. The semicircles of Nyquist plots have been fitted to demonstrate the accurate R_{ct} values with (b) corresponding equivalent circuit diagram. R_s, CPE and R_{ct} represent solution resistance, constant phase angle element and faraday impedance, respectively.

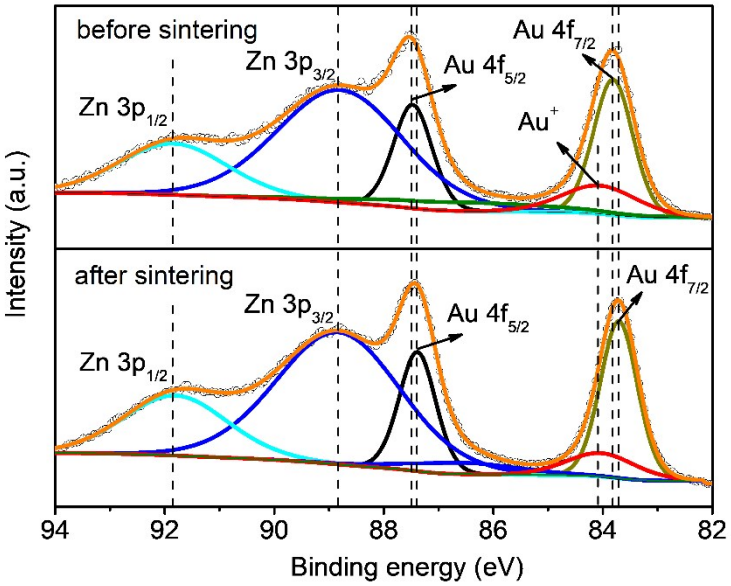

Fig. S12 XPS spectra of Au 4f and Zn 3p from the surface of $Au_{0.75}$/ZnO before and after 500 ^{o}C calcination.

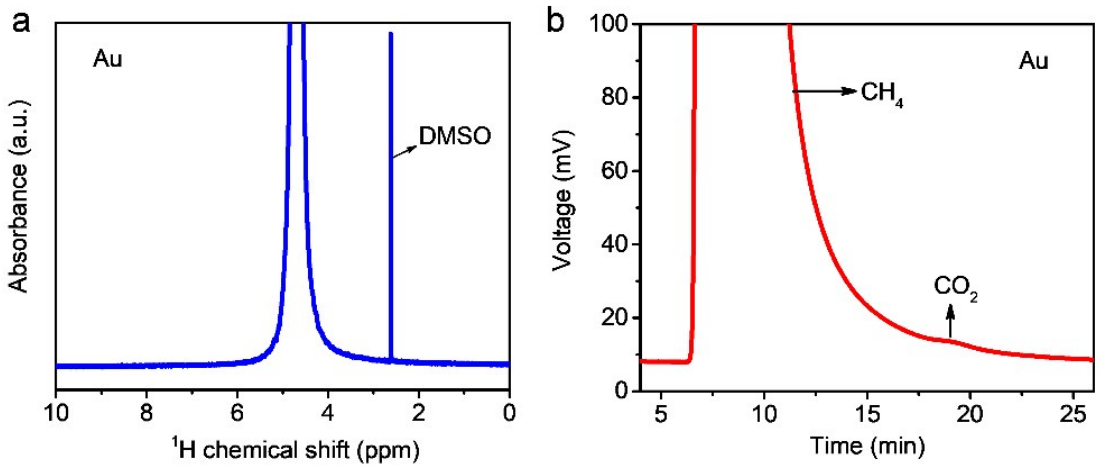

Fig. S13 (a) No liquid product has been found in ^{1}H NMR spectrum taking Au as photocatalyst. DMSO was added as internal standard in NMR test. (b) GC spectrum of the gas phase product taking Au as photocatalyst, and only 0.2 μmol g^{-1} of CO_2 has been observed.

For photocatalytic CH_4 oxidation, 10 mg of Au sample was suspended in 10 mL deionized water under stirring. The reactor was sealed and purged with a CH_4/O_2 mixing gas with 15 and 5 bar, respectively. During the light irradiation (2h), the reaction temperature was maintained at 30 ^oC using a cooling water bath. After photocatalytic CH_4 reaction, the liquid and gas products were collected and tested by NMR and GC spectra, respectively. No liquid product and only 0.2 μmol g^{-1} of CO_2 have been found as shown in Fig. S13a, b.

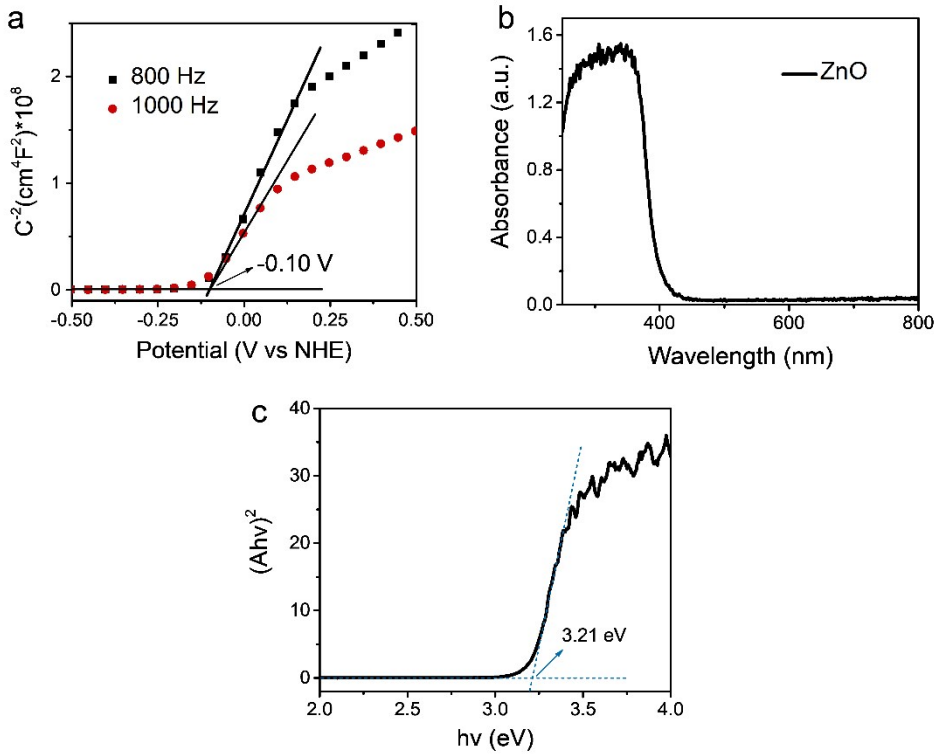

Fig. S14 (a) Mott-Schottky curves of ZnO under frequencies of 800 and 1000 Hz. (b) UV-Vis diffuse reflectance spectrum of pristine ZnO with (c) the transformed Kubelka-Munk plot, respectively.

The band structure of ZnO has been accurately explore through Mott-Schottky plots (Fig.S14a), UV-Vis diffuse reflectance spectra (Fig.S14b) and transformed Kubelka-Munk function plots (Fig.S14c). Bandgap value of ZnO is calculated to be 3.21 V vs. NHE via Kubelka-Munk function plot in Fig. S14c, which transformed from the UV-Vis absorption spectra in Fig. S14b. Flat conduction band potential of ZnO is revealed to be -0.10 eV vs. NHE through Mott-Schottky plots at frequencies 800 Hz and 1000 Hz in Fig. S14a. Then, deriving from the values between flat conduction band and bandgap, the valence band potential of ZnO is calculated be to 3.11 V vs. NHE.

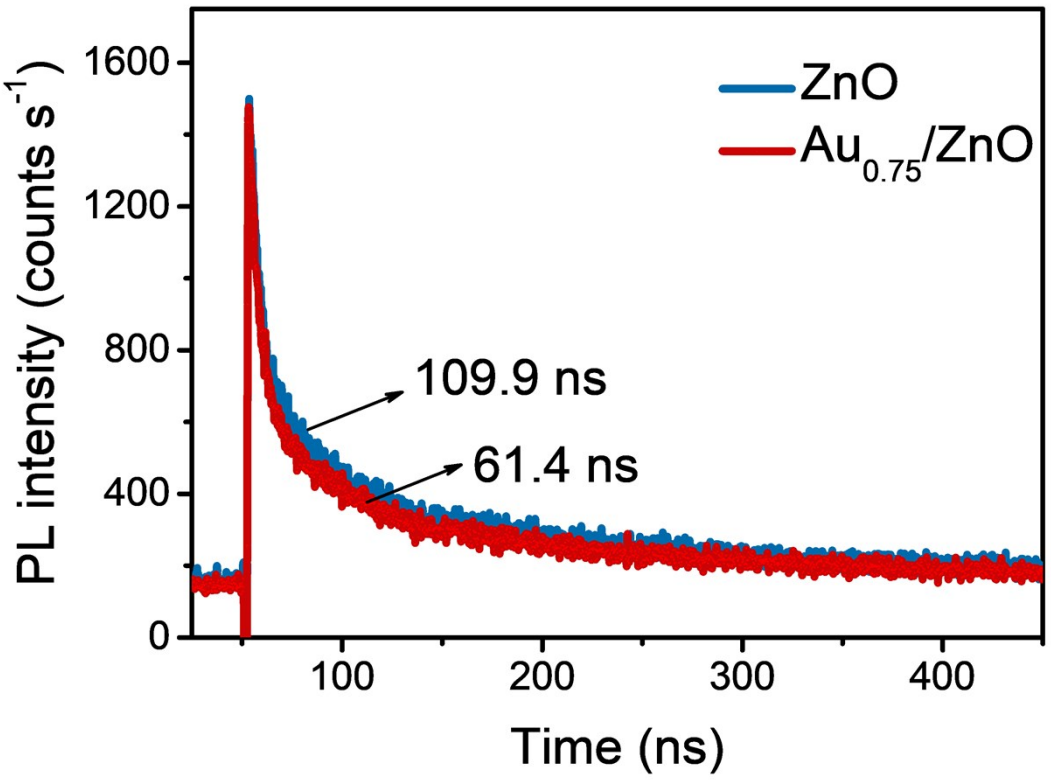

Fig. S15 (a) Time-resolved PL spectra for fresh ZnO and $Au_{0.75}$/ZnO nanocrystals under 344 nm excitation.

Comparing to ZnO (109.9 ns), the descent of emission lifetime of $Au_{0.75}$/ZnO (61.4 ns) is attributed to the decreased conduction electrons within ZnO, which has been transferred into adjacent Au.

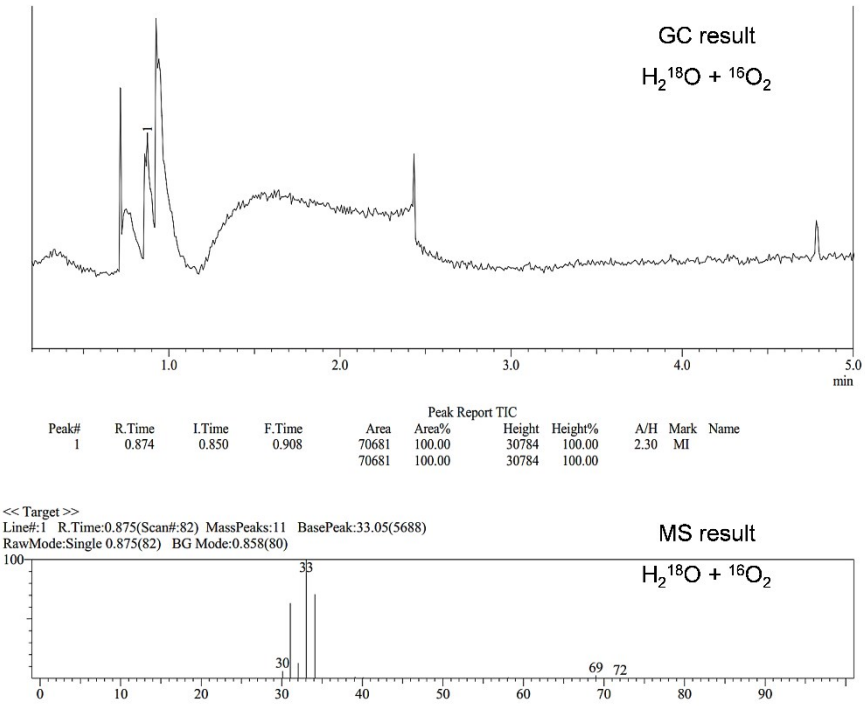

Peak Report TIC

Peak#	R.Time	I.Time	F.Time	Area	Area%	Height	Height%	A/H	Mark	Name
1	0.874	0.850	0.908	70681	100.00	30784	100.00	2.30	MI	
				70681	100.00	30784	100.00			

Fig. S16 Primary results of GC-MS analyses in $H_2{}^{18}O + {}^{16}O_2$ system.

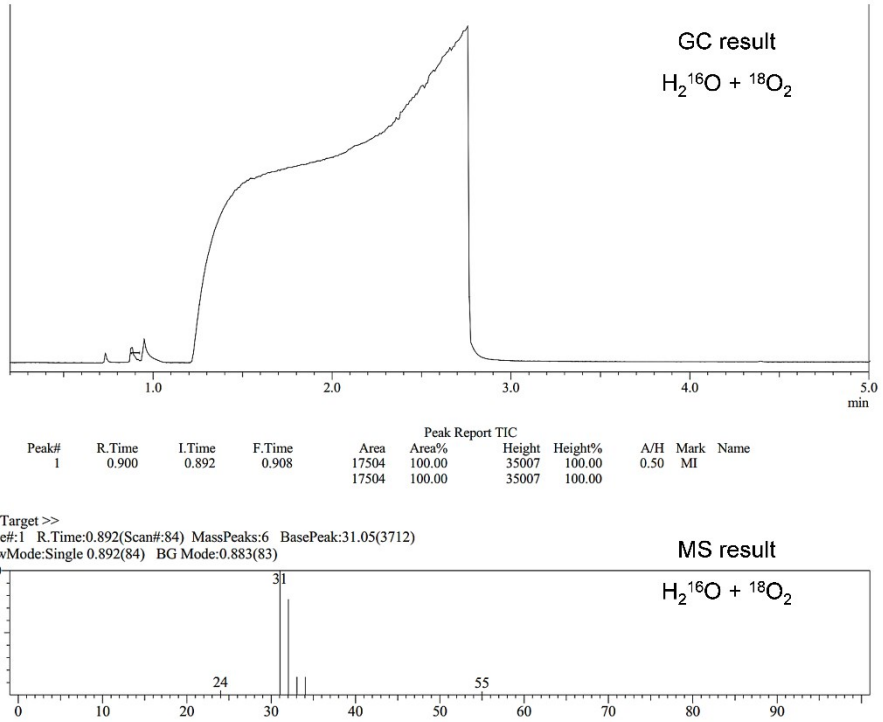

Peak Report TIC

Peak#	R.Time	I.Time	F.Time	Area	Area%	Height	Height%	A/H	Mark	Name
1	0.900	0.892	0.908	17504	100.00	35007	100.00	0.50	MI	
				17504	100.00	35007	100.00			

Fig. S17 Primary results of GC-MS analyses in $H_2{}^{16}O + {}^{18}O_2$ system.

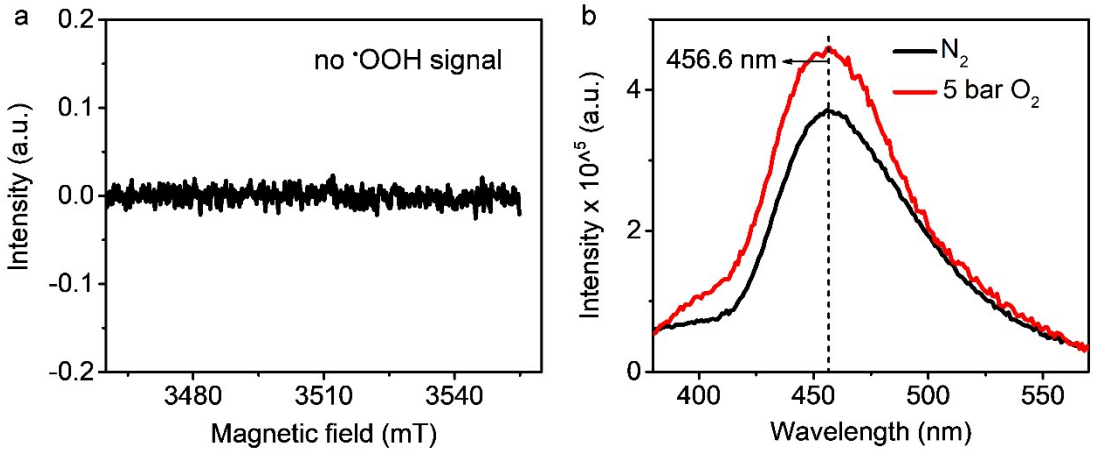

Fig. S18 (a) ESR spectrum of $Au_{0.75}$/ZnO with O_2 dissolved in methanol. DMPO has been added in solution as the radical trapping agent of ·OOH. (b) Fluorescence spectra of 1 mM coumarin solution over $Au_{0.75}$/ZnO with or without O_2 incorporation. The fluorescence peaks are located at 456.6 nm under 332 nm excitation.

Different from the reported work that O_2 was the only O-source of CH_3OH, we find that H_2O has provided more O-atoms than O_2 for the formation of CH_3OH. We think that the light source, including wavelength and light intensity, as well as the loading amount of Au should bear the most responsibility for the mechanistic differences. In our work, due to the lower energy input of light source (full light spectrum, 100 mW cm^{-2}, Fig. S6) than the previous report (UV irradiation, 100 mW cm^{-2})[1], O_2 can be more readily reduced to ·OH (0.695 V vs. NHE) rather than ·OOH (-0.046 V vs. NHE), as no ·OOH is observed in the ESR spectrum (Fig. S18a). Therefore, O_2 cannot engage in the formation of CH_3OH through the ·OOH path, which reduces the chance of O_2 as the O-source of CH_3OH. As mentioned above, ·OH plays two roles in the oxidation of CH_4, one is to active CH_4 into $·CH_3$ (step 2, Fig. 3), other is combined with $·CH_3$ to form CH_3OH (step 3, Fig. 3). And the ·OH can be produced through both H_2O oxidation and O_2 reduction. Thus, the separate contributions of ·OH generation, from H_2O oxidation or O_2 reduction, have been investigated by fluorescence spectra of coumarin solution with and without O_2 (Fig. S18b). From the peak intensity analysis of fluorescence spectra, we can find that O_2 offers less than 17.4 % enhancement in the formation of ·OH. This is because the consumption of electrons can accelerate the generation of holes to oxidize H_2O into ·OH. Thus, more than 82.6 % of ·OH is generated by H_2O oxidation. Therefore, the O-atom of CH_3OH mainly comes from H_2O as shown in the results of GC-MS (Fig. 6a). Since no CH_3OOH is observed in the products of $Au_{0.75}$/ZnO, we can deduce that little O_2 has engaged in the generation of CH_3OH through step 4. But step 4 is fitting for the generation of CH_3OH when the loading amount of Au less than 0.75 wt%.

Table S1. Comparisons of photocatalytic activities of ZnO and Au_x/ZnO (x= 0.08, 0.15, 0.30, 0.75, 1.57 and 1.79) for CH_4 conversion.

entry	photocatalyst	productivity (μmol g^{-1})			CH_3OH selectivity in liquid products (%)	CH_3OH selectivity in all products (%)
		CH_3OH	CH_3OOH	CO_2		
1	ZnO	178	135	0.5	56.9	56.8
2	$Au_{0.08}$/ZnO	343	297	0.8	53.6	53.5
3	$Au_{0.15}$/ZnO	951	1082	11.7	46.8	46.5
4	$Au_{0.30}$/ZnO	1996	407	12.2	83.1	82.7
5	$Au_{0.75}$/ZnO	1371	0	12.3	100	99.1
6	$Au_{1.57}$/ZnO	1197	0	13.2	100	98.9
7	$Au_{1.79}$/ZnO	1173	0	14.7	100	98.8

Reaction conditions: 10 mg catalyst, 10 mL H_2O, 5 bar O_2 and 15 bar CH_4, 30 °C reaction temperature, 2 h reaction time, light source: Xenon full light irradiation, light intensity 100 mW cm^{-2}. CH_3OH selectivity in liquid products (%) = productivity of CH_3OH × 100 / (productivity of CH_3OOH + productivity of CH_3OH). CH_3OH selectivity in all products (%) = productivity of CH_3OH × 100 / (productivity of CH_3OOH + productivity of CH_3OH + productivity of CO_2).

Table S2. The comparisons of CH_3OH selectivities over $Au_{0.75}/ZnO$ with other reported photocatalysts.

catalyst	reaction condition			CH_3OH productivity ($\mu mol\ g^{-1}$)	STY of CH_3OH ($\mu mol\ g^{-1}\ h^{-1}$)	CH_3OH selectivity (%)	ref.
	reactants	T (^oC)	light				
$Au_{0.75}/ZnO$	P_{CH_4} = 15 bar; P_{O_2} = 5 bar; *Cat.*: 10 mg	30	300 nm < λ < 1200 nm; light intensity 100 mW cm^{-2}	1371	685.5	99.1	My work
0.1 wt % Au/ZnO	P_{CH_4} = 20 bar; P_{O_2} = 1 bar; *Cat.*: 10 mg	25 ± 2	300 nm < λ < 500 nm; light intensity 100 mW cm^{-2}	4120	2060	15.7	*J. Am. Chem. Soc.* 2019, **141**, 20507-20515
Cu-0.5/ PCN	P_{CH_4} = 1 bar; *Cat.*: 20 mg	room temperature	visible light	24.5	24.5	18.8	*Nat. Commun.* 2019, **10**, 506
0.33 metal wt.% FeO_x/ TiO_2	P_{CH_4} = 1 bar; $V_{H_2O_2}$ = 4 mL; *Cat.*: 10 mg	25	300 nm < λ < 710 nm	1056	352	90	*Nat. Catal.* 2018, **1**, 889–896
WO_3/La	P_{CH_4} = 1 bar; *Cat.*: 0.3 g	55	medium-pressure Hg lamp	~ 64.7	~32.3	~47.1	*Appl. Catal. B-Environ.* 2016, **187**, 30-36
Ag–ZnO	78.9% N_2, 21.1% O_2 and 100 p.p.m. CH_4; *Cat.*: 0.5 g	0 or 80	300 nm < λ < 1200 nm; light intensity 200 mW cm^{-2}	none	none	none	*Nat. Commun.* 2016, **7**, 12273-12280

STY: a space-time yield is a vital benchmark for CH_3OH yield assessment taken reaction time into consideration. Though lower productivity of CH_3OH is obtained in our work compared to that of *J. Am. Chem. Soc.* 2019, **141**, 20507-20515, the selectivity is highest with 99.11 %, and the reaction conditions are much milder with low CH_4 pressure and applicable light irradiation range.

References

1. H. Song, X. Meng, S. Wang, W. Zhou, X. Wang, T. Kako and J. Ye, *J. Am. Chem. Soc.*, 2019, **141**, 20507-20515.